JOURNAL OF MATERIALS SCIENCE: MATERIALS IN MEDICINE **16** (2005) 899–907

Effect of carbonate substitution on the ultrastructural characteristics of hydroxyapatite implants

A. PORTER[1,*], N. PATEL[1], R. BROOKS[2], S. BEST[1], N. RUSHTON[2], W. BONFIELD[1]
[1]*Department of Materials Science and Metallurgy, University of Cambridge, Pembroke Street, Cambridge, CB2 3QZ, UK*
[2]*Orthopaedic Research Unit, University of Cambridge, Box 180, Addenbrooke's Hospital, Hills Road, Cambridge, CB2 2QQ*
E-mail: aep30@cam.ac.uk

Carbonate ion substitution has been shown to be beneficial for increasing the amount of *in vivo* osseointegration to hydroxyapatite (HA). Nevertheless, mechanisms by which carbonate ions increase *in vivo* bioactivity are not fully understood. Sintered granules of HA and carbonate-substituted hydroxyapatite (CHA) were implanted for 6 and 12 weeks in an *ovine* model. Samples containing the bone-implant interface were prepared for transmission electron microscopy (TEM) and TEM was used to compare the *in vivo* reactivity of sintered granules of HA and CHA.

The current findings demonstrated that CHA (1.2 and 2.05 wt.%) is more soluble than pure HA *in vivo*. More dissolution was observed from the CHA, at the bone-implant interface and within the implant, when compared to pure HA. A less crystalline phase was formed between the 2.05 wt.% CHA and bone at 12 weeks *in vivo*. Bone surrounding both the pure HA and 1.2 wt.% CHA was relatively disorganised at 12 weeks. In comparison, bone surrounding the 2.05 wt.% CHA was considerably more organised and in many regions collagen fibrils were present. Despite increased quality of bone surrounding 2.05 wt.% CHA, compared to 1.2 wt.% CHA, the amount of dissolution from both materials was similar.

1. Introduction

The rationale for the development of synthetic apatites for use in clinical orthopaedic applications has stemmed from their close chemical similarity to the inorganic phases of natural hard tissues. In adopting this biomimetic approach, synthetic hydroxyapatite [$Ca_{10}(PO_4)_6(OH)_2$; HA] has been widely studied as a bone substitute material. Although HA has been used as a graft material for a number of medical applications, the rate at which bone apposes HA surfaces is relatively slow compared to some bioactive glasses and glass-ceramics [1, 2].

A potential method of producing synthetic HA with enhanced osseointegration is to incorporate ions that are present in bone mineral, such as carbonate ions, into the HA structure. In addition to calcium, phosphate and hydroxyl ions, the inorganic component of hard tissues contains a significant proportion of carbonate ions (2–8 wt.%) [3]. Although the levels of carbonate ions in bone mineral are small, studies have demonstrated that these ions may play a significant role in the biochemistry of hard tissues [3, 4]. Consequently, a number of studies have focussed on the production of synthetic carbonate-substituted hydroxyapatite (CHA) ceramics for bone replacement [5–8]. The bulk of these studies have concentrated on the effects of carbonate-substitution on the chemical, structural and physical aspects of HA [4, 7, 9, 10]. Carbonate ion substitution has the effect of inducing lower crystallinity (i.e. crystallite size) and a higher number of structural defects within the HA structure [11, 12]. TEM studies by LeGeros *et al.* have indicated that crystallite morphology changes from needle-like to more equiaxed with increasing carbonate ion substitution [4]. In addition, the substitution of carbonate ions has the effect of reducing the sintering temperature required to achieve near-theoretical density [5, 7–9] and that decreased sintering temperatures had the effect of reducing the grain size of the resulting ceramic when compared to stoichiometric HA [5, 13].

The effects of carbonate substitution on the biological performance of HA are not fully understood, although *in vitro* experiments have demonstrated that carbonate substitution increases solubility and improves the bioactivity of HA [7–9, 14, 15]. The increased

*Author to whom all correspondence should be addressed.

solubility and *in vivo* bioactivity of CHA ceramics may be related to the effects of carbonate ion substitution on the physical characteristics of HA. For example, Merry investigated the effects of carbonate-substitution and grain size on the *in vitro* bioactivity of HA using simulated body fluid (SBF) solutions [9]. The results from this study indicated that the time required to form a poorly crystalline "bone-like" apatite layer on the surface of 8.2 and 11.3 wt.% CHA (grain size 2–3 μm) was approximately 2 days compared to 21 days for stoichiometric HA (grain size 5–6 μm) samples. The accelerated rates of formation of a "bone-like" apatite layer with carbonate ion substitution were reported to arise due to a chemical effect and to subsequent processing and sintering conditions, where formation of the apatite layer increased with decreasing grain size [9]. In a similar study, Gibson and Bonfield reported that the time required to form a "bone-like" apatite layer on the surface of 3.2 wt.% CHA samples immersed in SBF solution was 7 days compared to 24 days for stoichiometric HA [7]. Furthermore, Doi *et al.*, observed that osteoclasts cultured from neonatal rabbits resorbed bone and sintered 3.8 and 5.8 wt.% CHA, but not sintered HA samples, suggesting that sintered CHA samples have characteristics that can be favourably compared with those of bone [8].

To date, the number of studies comparing the *in vivo* response of HA and CHA ceramics are limited. Ellies *et al.* observed that the quantity of intermedullary bone formed around dense 3 and 6 wt.% CHA ceramic implants in rat femurs increased with carbonate content [16]. However, quantitative analysis of implant dissolution was not reported and just one implantation time of 4 weeks was investigated. In contrast, Barralet *et al.,* reported that the dissolution rate of 3.2 wt.% CHA was in the order of 5 times that of HA when subcutaneously implanted in Wistar rats for 10 weeks [10].

Recent studies in our research group have demonstrated that the percentage of bone ingrowth for pure HA and CHA (1.2 and 2.05 wt.%) granules followed the order 2.05 wt.% CHA > 1.2 wt.% CHA > pure HA, when implanted into the femoral condyle of an *ovine* model for 6 and 12 weeks [13]. In addition, histology images highlighted an increased presence of multinucleated "osteoclast-like" cells resorbing the surface of CHA implants.

Although these *in vitro* and *in vivo* studies have demonstrated the enhanced bioactivity of CHA ceramics, the mechanisms by which this process occurs are still not resolved; in particular the mechanism(s) underlying the physiological degradation behaviour of CHA ceramics are not clear. The main objective of this study was to use high-resolution transmission electron microscopy (HR-TEM) to investigate the dissolution and bone apposition of CHA granules *in vivo*. Similar studies on silicate-substituted hydroxyapatite (Si-HA) ceramics have demonstrated that the enhanced bioactivity of Si-HA was related to the presence of an increased number of defects in the ceramic compared to stoichiometric HA [17, 18]. In this study, it is hypothesised that the substitution of carbonate ions into the HA lattice increases its bioactivity by increasing the number of triple-junction grain boundaries. The grain boundaries are the specific sites within the HA ceramic that are most vulnerable to dissolution. Therefore, by increasing the number of grain boundaries the solubility of the HA ceramic in a biological environment is increased, as is its rate of osseointegration.

2. Materials and methods

2.1. Chemical synthesis

Stoichiometric HA, with a calcium/phosphorus (Ca/P) molar ratio of 1.67, was prepared by a precipitation reaction between calcium hydroxide, $Ca(OH)_2$, and orthophosphoric acid, H_3PO_4, solutions according to methods described elsewhere [19]. Precipitation occurred when the H_3PO_4 solution was dripped continuously into the $Ca(OH)_2$ solution at ambient temperature. The pH of the reaction was maintained at 10.5 with the addition of ammonia solution.

Concentrations of 1.20 and 2.05 wt.% CHA were prepared in a similar manner to HA, but in addition to $Ca(OH)_2$ and H_3PO_4 solutions, carbonate ions were introduced by bubbling carbon dioxide (CO_2) gas into the reaction vessel prior to the precipitation reaction [7].

The resulting filter-cakes of HA, 1.20 wt.% CHA and 2.05 wt.% CHA were processed into green granules (1–2 mm in diameter) by partial grinding and mechanical sieving. The HA granules were sintered at 1200 °C for 2 h in air and the 1.20 wt.% CHA and 2.05 wt.% CHA granules were sintered for 2 h in a moist CO_2 atmosphere at 1050 and 950 °C, respectively.

The sintered granules underwent full structural characterisation, prior to implantation [13]. X-ray diffraction and X-ray fluorescence spectroscopy analyses confirmed phase and chemical purity of the samples [13]. Scanning electron microscopy studies and image analysis of the microstructures indicated that the grain size of 1.20 wt.% CHA and 2.05 wt.% CHA were significantly smaller than HA [13]. Previous studies on the absolute density and grain size of sintered HA, 1.20 wt.% CHA and 2.05 wt.% CHA are summarised in Table I.

2.2. *In vivo* model and tissue processing

The guidelines for the care and use of laboratory animals (Animals (Scientific Procedures) Act 1986) were observed throughout the implantation procedures. The sintered granules of stoichiometric HA, 1.20 wt.% CHA and 2.05 wt.% CHA were implanted into 2–3 year old Texcel x Continental sheep weighing between 70–80 kg. Implants were placed bilaterally into the femoral condyle. This site was selected as it presented a large

TABLE I Physical properties of HA, 1.20 wt.% and 2.05 wt.% CHA implants [13]

Sample	Absolute density (g/cm^3)	Mean grain size (μm)
HA	3.047 ± 0.007	1.11 ± 0.53
1.20 wt.% CHA	3.070 ± 0.008	0.33 ± 0.11
2.05 wt.% CHA	3.118 ± 0.010	0.24 ± 0.11

volume of load bearing cancellous bone within the animal. An incision was made adjacent to the femoral condyle and the soft tissue was dissected to reveal the bone. A defect 0.9 cm in diameter and 0.9 cm in depth was drilled into the bone and washed with sterile saline solution. The defect was filled with the granular implant material and the subcutaneous tissues and skin were subsequently sutured, encapsulating the granules. Both implant compositions were studied at two time points: 6 and 12 weeks.

Following sacrifice, sections containing the bone-HA/CHA interface were sawn and trimmed. The specimens were fixed in ethylene glycol for 24 h from the time of trimming and were rinsed in 100% ethanol twice for 5 min. The specimens were infiltrated with Spurr's resin (Agar Scientific, Essex, UK) over several days: Spurr's resin was prepared with 10 g epoxy monomer vinyl cyclohexene dioxide (ERL), 4.5 g diglycidyl ether of polypropylene glycol (DER-736), 26 g nonenyl succinic anhydride (NSA) and 0.7 g benlybimethylamine (BDMA). The samples were agitated at room temperature in 1:1 solutions in propylene oxide:Spurr's for 2 days, 1:3 propylene oxide:Spurr's for 1 day, then 100% Spurr's for 2 weeks under vacuum. The Spurr's resin was changed every 24 h. Samples were then cured in fresh Spurr's resin for 23 h at 60 °C.

2.3. Preparation for microscopy

Silver to gold sections (70–90 nm) containing the bone/HA and bone/CHA (1.2 and 2.05 wt.%) interface, were cut onto distilled water with an ultramicrotome using a 45° diamond knife. Sections were collected immediately on lacey carbon 300 mesh copper grids and dried for an hour at 37 °C. Selected sections were decalcified on 1% EDTA, for 10 min then stained in uranyl acetate and lead citrate. The grids were placed sample side down on individual drops of 2% uranyl acetate in 50% ethanol for 10 min in a light-tight box. Other selected thin sections were stained with lead citrate and uranyl acetate for 10 min in each.

2.4. Transmission electron microscopy

TEM and selected area electron diffraction (SAED) were performed in the Philips CM30 operated at 300 kV. Diffraction contrast was employed for the bright-field imaging.

3. Results

3.1. Transmission electron microscopy observations

3.1.1. Pure HA

Low magnification images of the bone/pure HA interface after 6 weeks *in vivo* revealed densely mineralised, disordered bone in the vicinity of the HA grains (Fig. 1(a)). However, many regions of interface were devoid of apatite crystallites. Decalcification and staining illustrated disorganisation of the collagen fibrils in the vicinity of the implant (Fig. 1(b)). In general dissolution from the pure HA was negligible at 6 weeks

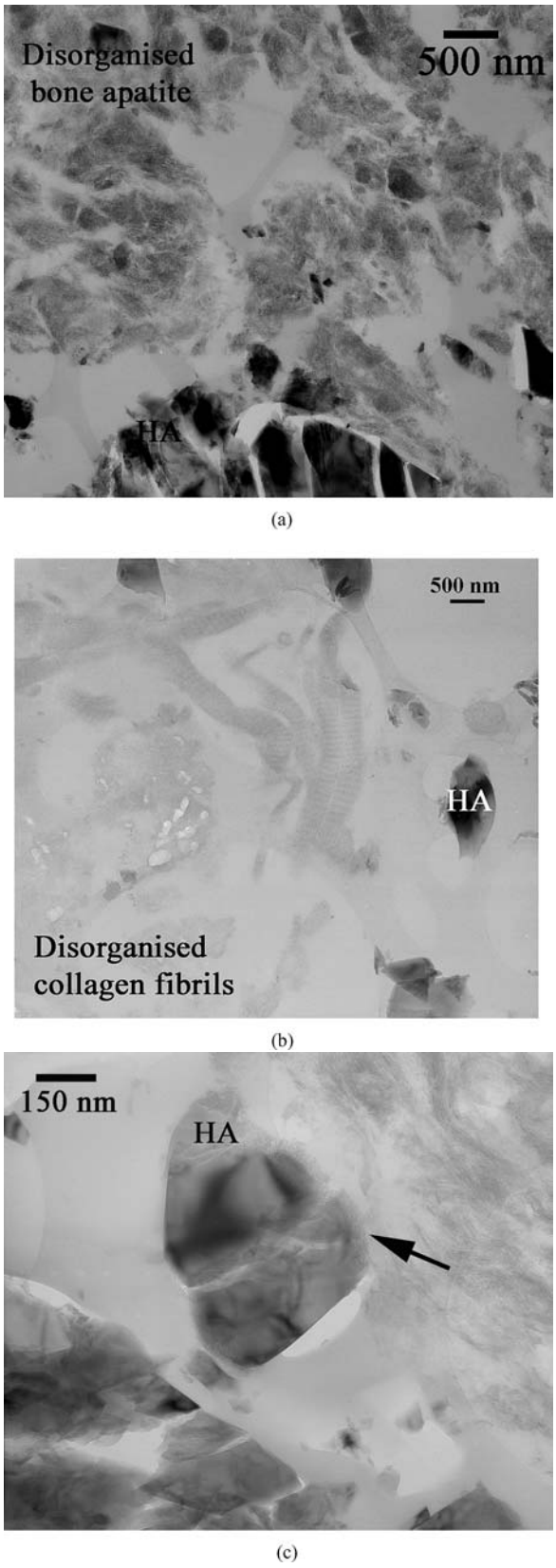

Figure 1 TEM micrographs of the interface between pure HA and bone at 6 weeks *in vivo*. (a) Densely mineralised, disordered bone directly abutting and near the HA. (b) Decalcified and stained section illustrating disorganisation of collagen fibrils in the vicinity of the implant. (c) Arrow indicating dissolving CHA at the bone-implant interface.

in vivo. Only one grain at the bone-HA interface displayed a small amount of degradation (Fig. 1(c)).

After 12 weeks *in vivo*, poorly organised bone surrounded the HA (Fig. 2(a)), with gaps appearing

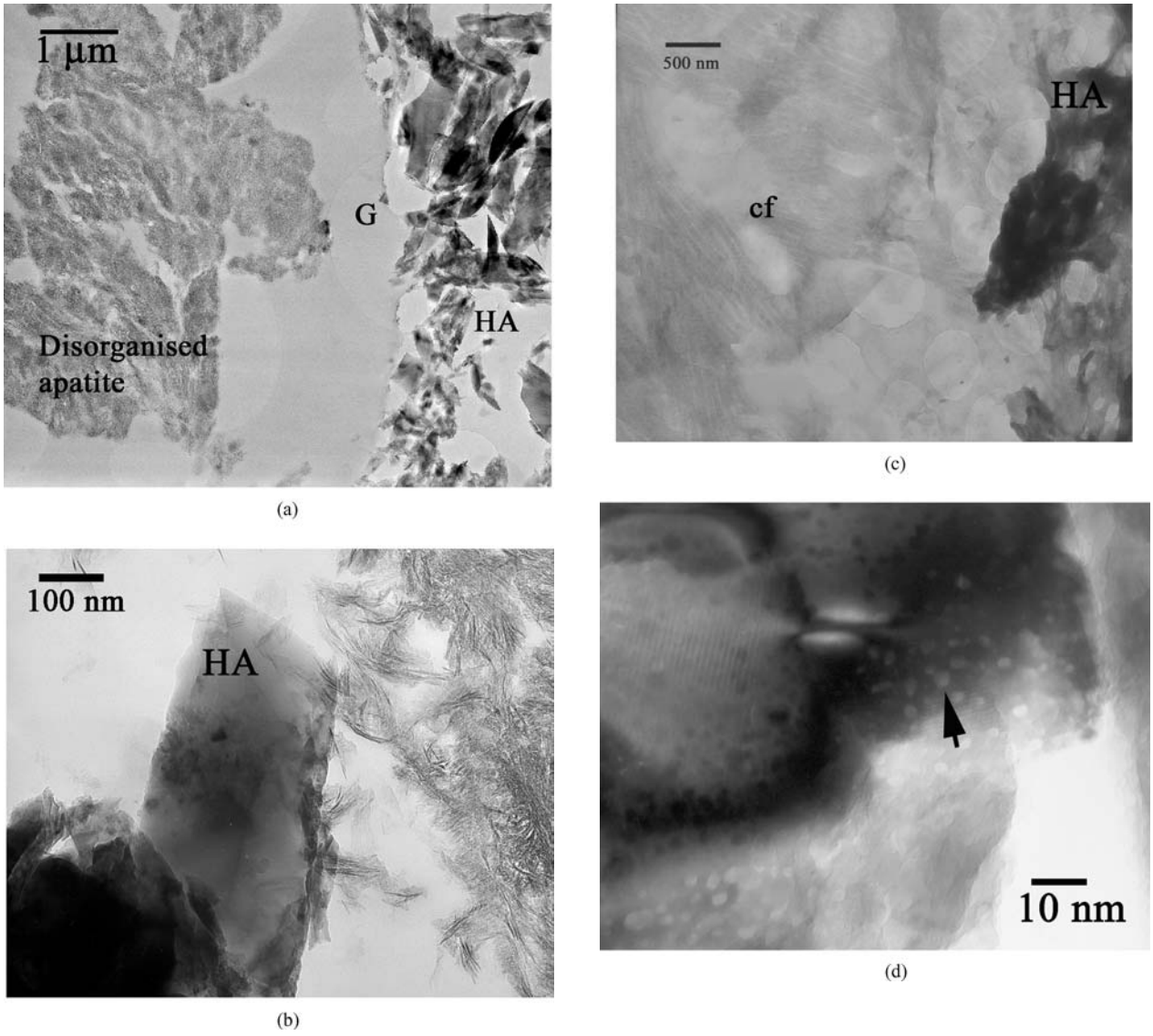

Figure 2 TEM micrographs of the pure HA-bone interface at 12 weeks *in vivo.* (a) Gap (G) between the HA and disorganized bone apatite at the bone/HA interface. (b) Densely mineralized, plate-like apatite directly abutting the HA (c) Decalcified and stained section, illustrating a more organised pattern of collagen fibrils (cf) than seen at 6 weeks *in vivo.* (d) Higher magnification micrograph of a pure HA grain. Arrow shows electrolucent spots, possibly related to dissolution.

between the apatite and the implant. In a few areas, densely mineralised plate-like apatite directly abutted the HA (Fig. 2(b)). Some regions also showed decalcification and staining revealed organised collagen fibrils surrounding the implant (Fig. 2(c)). Lower magnification imaging revealed no signs of dissolution from the HA, whereas higher magnification imaging illustrated many voids on the surface of grains within the implant (Fig. 2(d)). The contrast of these voids suggested that they were related to a loss of mineral, which could be associated with early stages of dissolution from the HA ceramic.

3.1.2. 1.2 wt.% CHA

Several sections of the 1.2 wt.% CHA had to be cut before regions containing the bone/CHA interface were found. In general, few areas of the implant were closely apposed by bone (where bone apposition is defined as a continuum of mineral from the bone to the HA). In the regions where bone apposed the implant, the bone mineral was densely mineralised and characterized by relatively poor organisation (Fig. 3(a)–(c)). Degradation of the 1.2 wt.% CHA was observed at the bone/implant interface at 6 weeks (Fig. 3(b) and (c)).

Many triple-junctions and grain boundaries were observed in the 1.2 wt.% CHA (Fig. 3(d)). After 12 weeks *in vivo,* extensive dissolution of the 1.2 wt.% CHA grains had occurred within the implant (Fig. 3(d) and (e)). Needle-like apatite crystallites emanated from the surface of the CHA grains and appeared to be connected to the 1.2 wt.% CHA grains by an interfacial region with a mottled appearance (Fig. 3(f)). Grain boundary dissolution was observed frequently in many of the crystallites (Fig. 3(f)). At several triple-junctions, an entire grain had dissolved away (Fig. 3(g)).

3.1.3. 2.05 wt.% CHA

At 6 weeks *in vivo*, dissolution was extensive and was observed at the grain boundaries (Fig. 4(a)). Bone at the implant/tissue interface was more organised than bone

surrounding the 1.2 wt.% CHA at 6 weeks. Organised collagen fibrils with a characteristic 67 nm banding pattern directly abutted the implant (non-stained section) (Fig. 4(b)).

At 12 weeks *in vivo*, many more regions of the implant were invaded by bone and organised collagen was observed with the characteristic 64 nm banding pattern (Fig. 5(a)). Along several regions of interface, the CHA displayed a mottled appearance indicating that signs of dissolution had occurred (Fig. 5(b)). Interestingly, along some regions of the interface, less organised apatite was found between the implant and the more organised bone (Fig. 5(c)). SAED confirmed the lack of organisation of the mineral in this region. In regions within the implant, some grains displayed a mottled appearance suggesting dissolution had occurred (Fig. 5(d)). After staining, collagen fibrils were revealed abutting and also in the region surrounding the implant (Fig. 5(e)). In many regions a gap was observed between the implant and the surrounding bone (Fig. 5(e)).

4. Discussion

Patel *et al*. recently demonstrated the beneficial effects of carbonate ion substitution on the amount of *in vivo* osseointegration to HA [13]. Nevertheless, the mechanisms by which these ions increase *in vivo* bioactivity are not fully understood. The consensus view in the literature suggests that the "bone bonding" ability of calcium phosphate ceramics occurs by the partial dissolution of the ceramic, resulting in elevated concentrations of calcium (Ca^{2+}) and phosphate (PO_4^{3-}) ions within the local environment. Subsequently, the released Ca^{2+} and PO_4^{3-} ions, combine with carbonate (CO_3^{2-}) ions and proteins from the biological milieu precipitate resulting in an intermediate apatite-like layer that forms on the surface of the implant *in vivo* [20, 21]. Consequently, it has been speculated that osteoblasts can preferentially proliferate and differentiate on this apatite-like layer [21]. Since the formation of an apatite-like layer is related to the surface reactivity of the implant, it seems reasonable to assume that the dissolution rates of calcium phosphate implants will influence the rate of formation of an apatite-like surface layer and in turn, influence bone formation on these surfaces.

Studies have reported that the physiological degradation processes of calcium phosphates are primarily influenced by the chemical composition, crystallinity, density, surface area and microstructure of the material [22, 23]. A previous HR-TEM study by Porter *et al*. suggested that enhanced bioactivity of HA compared to silicon substituted hydroxyapatite (Si-HA) resulted from an increased number of triple-junctions in the Si-HA compared to pure HA. The Si-HA study suggested that the increase in triple-junction density is significant as dissolution nucleates at this site [18]. *In vitro* findings by Doi *et al*. revealed accelerated dissolution around the CHA compared to the pure HA [8]. In addition, CHA would be expected to be more soluble than HA since the grain size of CHA is smaller than that of HA, therefore there would be a greater density of triple-junctions acting as nucleation sites for dissolution (at constant absolute density). The current findings also demonstrate that CHA (1.2 and 2.05 wt.%) are more soluble than pure HA *in vivo*. TEM observations highlighted dissolution

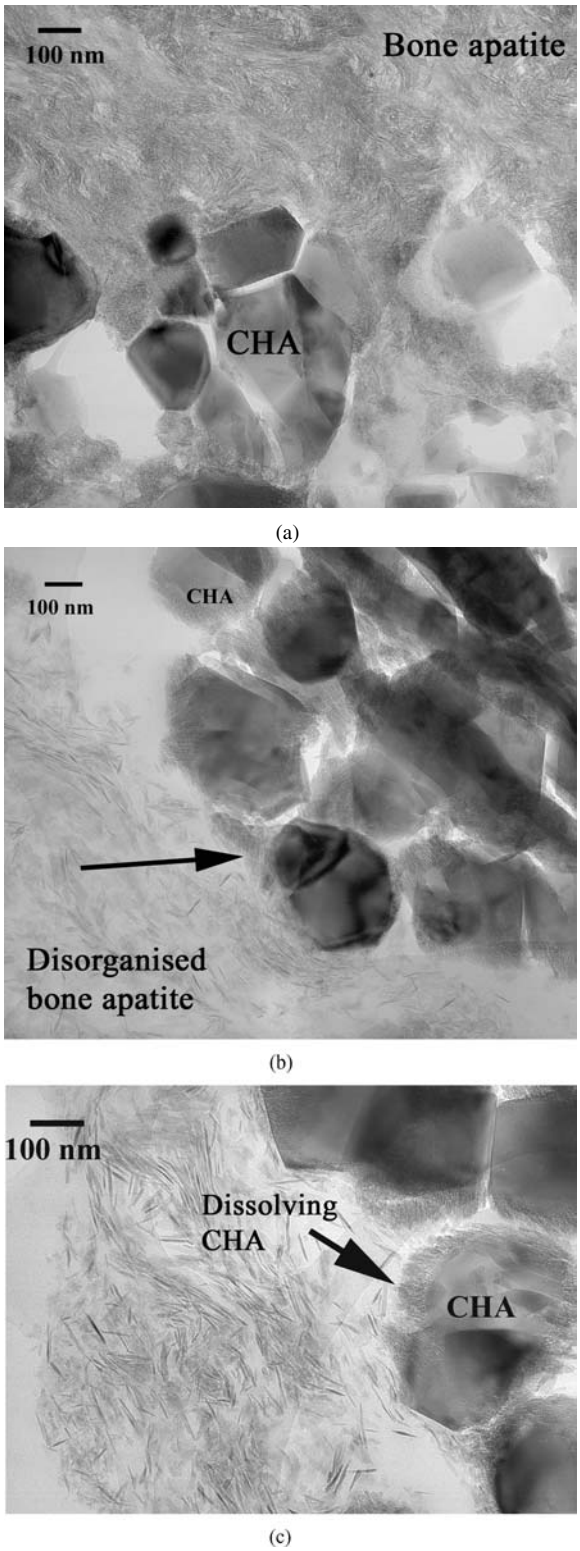

Figure 3 1.2 wt.% CHA after 12 weeks *in vivo*. (a) Densely mineralized, disorganised bone apatite surrounding the implant. (b, c) Dissolving CHA at the bone-implant interface (as indicated by the arrows). (d) Extensive dissolution of the CHA grains within the implant. Arrow indicates needle-like crystallites (n) emanating from the CHA and an interfacial region with a mottled appearance (m). (e) Needle-like crystallites emanating from the surfaces of the 1.2 wt.% CHA grains (as indicated by the arrow). (f) Grain boundary dissolution (as indicated by black arrow). (g) Dissolution of an entire grain at a triple junction of the 1.2 wt.% CHA (as indicated by arrow). (*Continued*.)

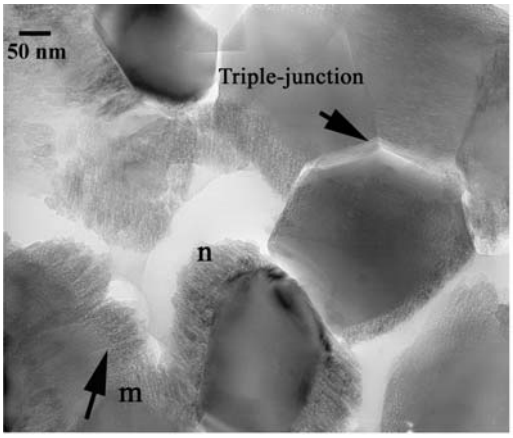

(d)

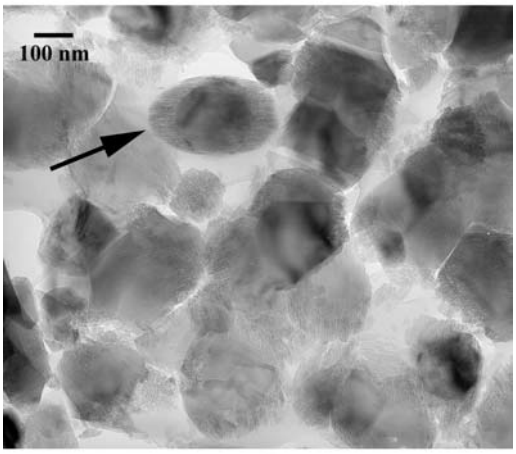

(e)

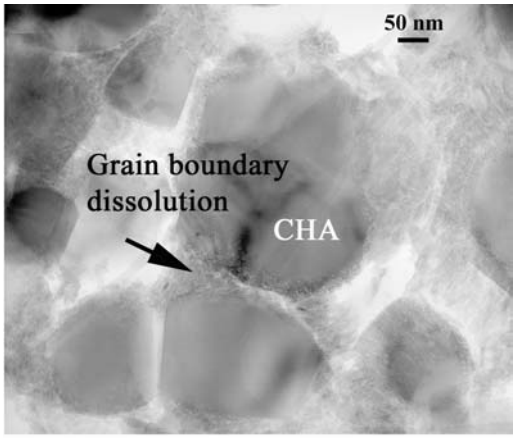

(f)

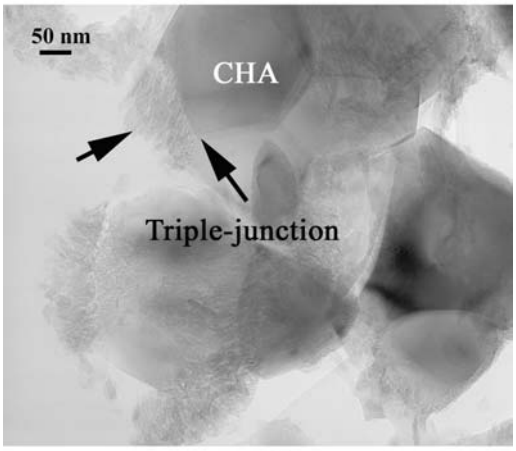

(g)

Figure 3 (*Continued*).

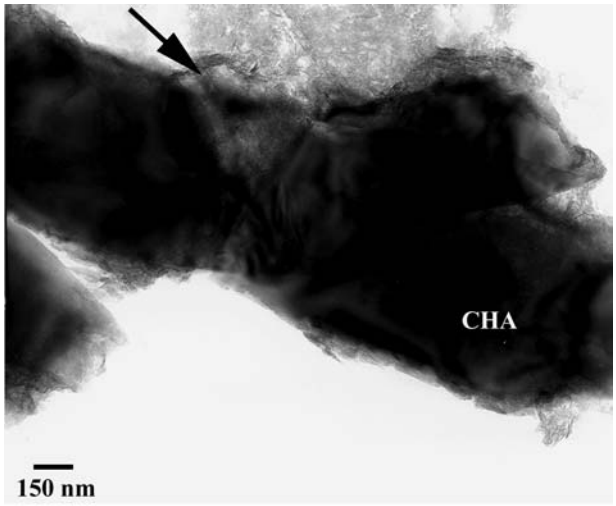

(a)

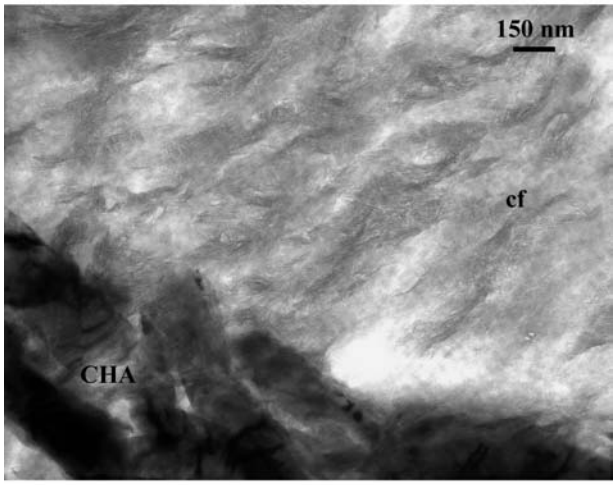

(b)

Figure 4 Ultrastructure of the 2.05 wt.% CHA implant/bone interface at 6 weeks *in vivo*. (a) Grain boundary dissolution (arrow). (b) Organised collagen fibrils (cf) with a characteristic 67 nm banding pattern directly abutting the CHA (non-stained section).

of the 1.2 and 2.05 wt% CHA at grain boundaries within the implant and also dissolution of the CHA at the bone-CHA interface. If bioactivity follows the commonly proposed, dissolution-reprecipitation mechanism [21], increased dissolution of CHA compared to pure HA may explain the increased amount of bone apposition to CHA [13].

Other evidence to suggest the increased solubility of CHA compared to pure HA was the observation of collagen directly abutting the 2.05 wt.% CHA surface with an interposed biological apatite layer, after 12 weeks *in vivo*. Reports in the literature have demonstrated the presence of collagen free [24] and apatite-rich layers [25] between bone and dense HA at shorter time periods. In the current study, more organized bone was found adjacent to a less organized biological apatite layer on the CHA. A study by Porter *et al*., investigating processes predisposing to bone bonding on plasma-sprayed HA coatings of different crystallinities, illustrated an interposed biological apatite layer on the coating of lower crystallinity (and hence higher solubility) [26]. The observation of this apatite layer further highlights the increased solubility of CHA over pure HA.

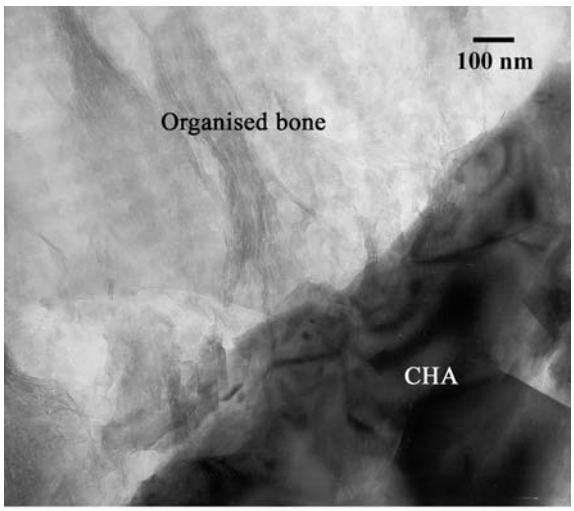

(a)

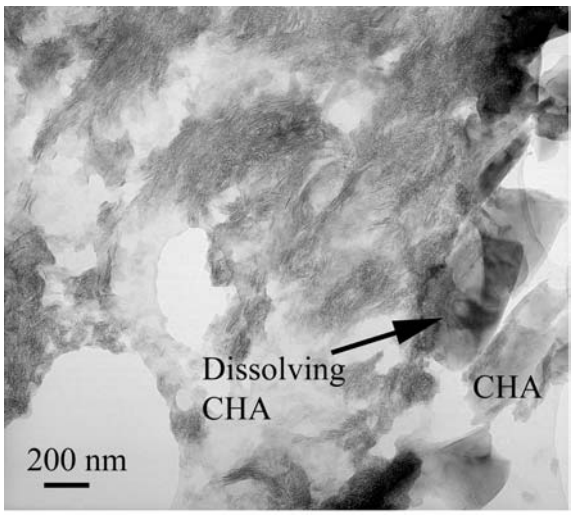

(b)

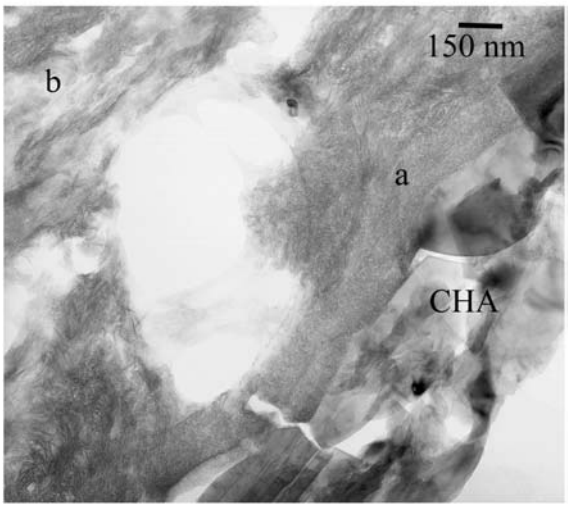

(c)

Figure 5 Ultrastructure of the 2.05 wt.% CHA implant/bone interface at 12 weeks *in vivo*. (a) Organised bone with a characteristic 67 nm banding pattern directly abutting the CHA (non-stained section). (b) Densely mineralized bone surrounding the 2.05 wt.% CHA implant. Arrow highlights mottled morphology, indicating dissolution of the CHA. (c) Arrow indicating a less organised apatite phase (a) between the implant and the more organised bone apatite (b). (d) Mottled appearance of grains within the implant indicating that some dissolution has occurred (as indicated by arrows). (e) Stained section indicating collagen fibrils (cf) in the region surrounding, but not directly abutting, the implant surface. (*Continued*.)

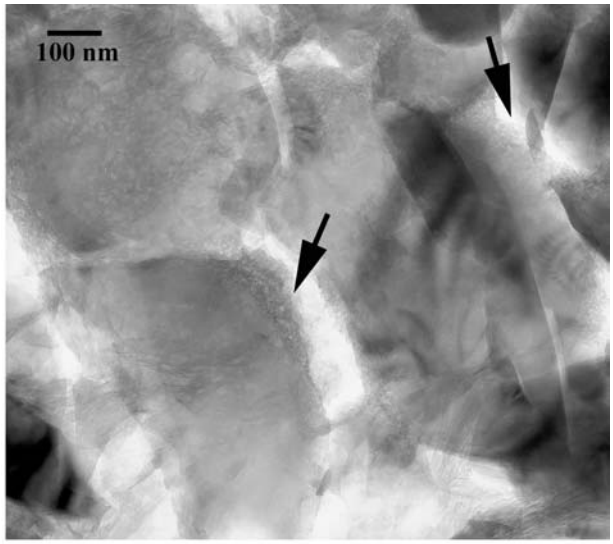

(d)

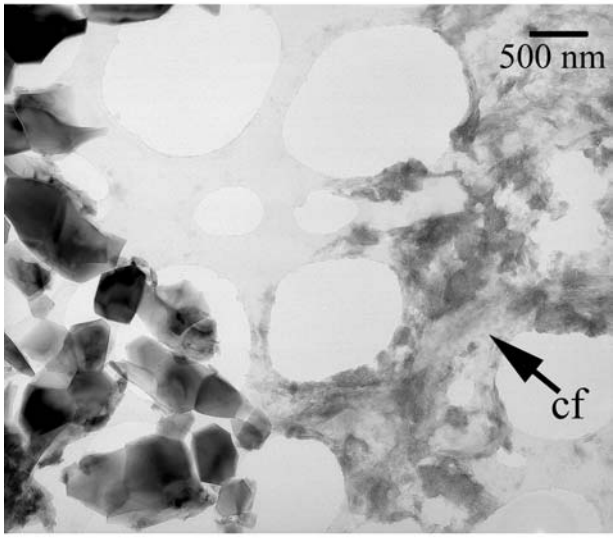

(e)

Figure 5 (*Continued*).

In attempting to explain increased solubility of CHA compared to pure HA, it has been proposed that the susceptibility of CHA towards dissolution could be attributed to its propensity towards osteoclastic cell-mediated resorption [8]. A study by Gomi *et al*. demonstrated that resorption pits (produced by osteoclast cells) were found on HA substrates with grain sizes larger than 100 nm, comparable to devitalized bone [27]. Webster *et al.* illustrated increased formation of resorption pits by osteoclast-like cells on nanophase (grain size less than 100 nm) HA [28]. In the present study, increased dissolution was observed from CHA compared to the pure HA. The increased resorption of CHA may be attributed to the increased solubility of CHA compared to pure HA. Investigations have suggested that there is a threshold concentration of calcium ions, released by acid secreted from the osteoclasts, required to stimulate the subsequent activity of osteoclasts [29, 30]. The current findings indicate that CHA first dissolves without the action of osteoclasts. The concentration of dissolution products may subsequently be sufficient to activate osteoclasts to cause further resorption.

An interesting finding in this study was that, despite increased solubility of CHA, organisation of bone surrounding the pure HA and 1.2 wt.% CHA at 12 weeks were similar. Disorganised bone apatite surrounded the pure HA and CHA (1.2 wt.%) at 12 weeks *in vivo* and in many regions, a gap was present between the implant and bone. A recent *in vitro* study by Hing *et al*., comparing the osteoblast response to HA and CHA (5.4–11.3 wt.%), established that the advantageous effect of CHA on bioactivity was only achieved at 8.2 wt.% CHA [14]. Schepers *et al*. demonstrated that the tissue response to a porous carbonated apatite material implanted in beagle mandibular bone was very similar to that with dense, stoichiometric HA [31]. Osseoconduction from the bone defect wall occurred over a limited distance and bone tissue conductions into the center of the defects were not observed. The lack of increased bioactivity of 1.2 wt.% CHA compared to HA may be attributed to increased solubility leading to degradation in the cell/substrate interface.

The current TEM observations suggest factors in addition to solubility must be considered to account for the increase in bioactivity associated with CHA. Findings illustrate that although more organised collagen fibrils surrounded 2.05 wt.% CHA than the 1.05 wt.% CHA at 12 weeks *in vivo*, there were no notable differences in solubility between the two materials. This is particularly surprising as the grain size of 2.05 wt.% CHA is smaller than that of 1.2 wt.% CHA [13, 15]. These findings suggest that other factors, such as surface topography, may modify implant bioactivity [28]. Webster *et al.* observed increased vitronectin and collagen on HA with yittrium (Y) doping and suggested that changes arose due to a modification in microtexture (decrease in grain size and increase in porosity) of HA with Y addition. The authors suggest that changes in microtexture lead to a conformational change of proteins on the surface of the HA which opens up the protein RGD sequence, thereby enhancing osteoblast attachment. The decrease in grain size of 2.05 wt.% CHA compared to 1.2 wt.% HA increases the density of topographical features, such as grain boundaries and triple junctions. This modification in surface topography may change the protein conformation and cellular attachment to the CHA implant surface. Hence, the effect of grain size on bioactivity is more complicated than simply its effect on solubility.

5. Conclusions

In conclusion, the present study has indicated that both 1.2 and 2.05 wt.% CHA are more soluble than pure HA. Despite increased solubility, the quality and amount of bone surrounding 1.2 wt.% CHA and pure HA are comparable at 6 weeks *in vivo*. In comparison, bone surrounding 2.05 wt.% CHA was more organised than either 1.2 wt.% CHA or pure HA. In many areas of the interface, a gap existed between the bone and the surrounding HA and CHA (1.2 and 2.05 wt.%) implants. Dissolution was significantly more prevalent from CHA, compared to pure HA, at the bone-CHA interface. Enhanced solubility of 1.2 and 2.05 wt.% CHA compared to pure HA is expected to be a result of the smaller grain size of CHA. It is suggested that CHA first dissolves without the action of osteoclasts but that the concentration of dissolution products is sufficient to activate osteoclasts to cause further resportion.

Acknowledgments

The authors would like to acknowledge the support of ApaTech Ltd. and the EPSRC.

References

1. N. IKEDA, K. KAWANABE and T. NAKAMURA, *Biomat.* **20** (1999) 1087.
2. H. OONNISHI, L. L. HENCH, J. WILSON, F. SUGIHARA, E. TSUJI, S. KUSHITANI and H. IWAKI, *J. Biomed. Mat. Res.* **44** (1999) 31.
3. F. C. M. DRIESSENS, *Bull. Soc. Chim. Belg.* **89** (1980) 663.
4. R. Z. LEGEROS, O. R. TRAUTZ, J. P. LEGEROS and E. KLEIN, *Science* **155** (3768) (1967) 1409.
5. J. BARRALLET, PhD Thesis, Materials Dept. QMW College, University of London, 1995.
6. J. BARRALLET, S. M. BEST and W. BONFIELD, *J. Mat. Sci.: Mat. Med.* **13** (2002) 529.
7. I. R. GIBSON and W. BONFIELD, *J. Biomed. Mat. Res.* **59** (2002) 697.
8. Y. DOI, T. SHIBUTANI, Y. MORIWAKE, T. KAJIMOTO and Y. IWAYAMA, *ibid.* **39** (1998) 603.
9. J. MERRY, PhD Thesis, Materials Dept. QMW College, University of London, 2000.
10. J. E. BARRALLET, M. AKAO and H. AOKI, *J. Biomed. Mat. Res.* **49** (1999) 176.
11. J. D. LAYANI, F. J. G. CUISNIER, P. STEUER, J. C. VOEGEL and I. MAYER, *ibid.* **50** (2000) 199.
12. R. Z. LEGEROS, in "Handbook of Experimental Aspects of Oral Biochemistry" (CRC Press, 1983) p. 159.
13. N. PATEL, PhD Thesis, University of Cambridge, 2003.
14. K. A. HING, J. METTER, I. R. GIBSON, I. R. DISILVIO, S. M. BEST and W. BONFIELD, in "Bioceramics," edited by H. Ohgushi, W. Q. Hastings, and T. Yoshikawa (World Scientific Publishing C. Pte. Ltd. Nara, Japan, 1999) Vol. 12 p. 195.
15. C. R. HANKERMEYER, K. L. OHASHI, D. C. DELANEY, J. ROSS and B. R. CONSTANTZ, *Biomat.* **23**(3) (2002) 743.
16. L. G. ELLIES, J. M. CARTER, M. NATIELLA, J. D. B. FEATHERSTONE and D. G. A. NELSON, *J. Biomed. Mat. Res.* **22** (1988) 137.
17. A. E. PORTER, S. M. BEST and W. BONFIELD, *ibid.* **24** (2003) 4609.
18. A. E. PORTER, N. PATEL, J. N. SKEPPER, S. M. BEST and W. BONFIELD, *Biomat.* **24** (2003) 4609.
19. M. AKAO, H. AOKI and K. KATO, *J. Mater. Sci.* **28** (1981) 809.
20. S. R. RADIN and P. DUCHEYNE, *J. Biomed. Mater. Res.* **27** (1993) 35.
21. P. DUCHEYNE and Q. QUI, *Biomat.* **20** (1999) 2287.
22. C. A. P. T. KLEIN, A. A. DRIESSEN, K. DE GROOT and A. VAN DEN HOOFF *J. Biomed. Mat. Res.* **17** (1982) 769.
23. K. DE GROOT, C. P. A. T. KLEIN and A. A. DRIESSEN, in Proceedings of the Institute of Mechanical Engineers (1998) Vol. 212(H) p. 137.
24. J. D. DE BRUIJN, J. S. FLACH, K. DE GROOT, C. A. VAN BLITTERSWIJK and J. E. DAVIES, *Cells Mater.* **3** (1993) 115.
25. M. NEO, S. KOTANI, T. NAKAMURA, T. YAMAMURO, C. OHTSUKI, T. KOKUBO and Y. BANDO, *J. Biomed. Mater. Res.* **26** (1992) 1419.
26. A. E. PORTER, L. W. HOBBS, V. BENEZRA ROSEN and M. SPECTOR, *Biomat.* **23** (2002) 725.

27. K. GOMI, B. LOWENBERG, G. SHAPIO and J. E. DAVIES, *ibid.* **14**(2) (1993) 91.
28. T. J. WEBSTER, C. ERGUN, R. H. DOREMUS, SIEGEL and R. BIZIOS, *ibid.* **22** (2001) 1327.
29. J. GLOWACHI, D. ALTOBELLI and A. J. MULLIIKEN, *Calcif. Tiss. Int.* **33** (1981) 71.
30. M. KRUKAOWSKI and A. J. KAHN, *ibid.* **34** (1982) 474.
31. E. SCHEPERS, M. DECLERCQ, P. DUCHEYNE and R. KEMPENEERS, *J. Oral. Rehab.* **18** (1991) 439.
32. T. J. WEBSTER, C. ERGUN, R. H. DOREMUS and R. BIZIOS, *J. Biomed. Mater. Res.* **59** (2002) 312.

Received 5 April
and accepted 17 November 2004